SMiRT-12 / K. Kussmaul (Editor)

E09/1

THE EFFECTS OF GEOMETRICAL IMPERFECTION ON BUCKLING STRENGTH OF CYLINDRICAL SHELLS IN BENDING

T. Murakami[1], H. Yoguchi[1], H. Hirayama[2], H. Nakamura[3] and S. Matsuura[3]

[1]Heavy Apparatus Engineering Lab., Toshiba Corporation, Yokohama, Japan
[2]Nuclear Energy Group, Toshiba Corporation, Yokohama, Japan
[3]Central Research Institute of Electric Power Industry, Chiba, Japan

ABSTRACT

Buckling tests for nearly perfect cylinders and cylinders with intentional imperfection made by press-working technique were carried out subjected to transverse shearing loads. The radius-to-thickness ratios were 50-200 and bending-to-shear stress ratios were 1.2-5.0, where both types of buckling in shear and in bending might occur. The purposes of these tests were to evaluate the interaction relation between elastic-plastic buckling strength in bending and in shear and to clarify the imperfection effect on these two types of buckling. From test results, we proposed a week interaction between buckling in shear and in bending and correction factors of buckling loads for larger imperfection in the interim buckling design guide of LMFBR.

1. INTRODUCTION

The Demonstration Test and Research Program of Buckling of FBR, commissioned by the Ministry of International Trade and Industry (MITI), has been made (1987-1993) by Central Research Institute of Electric Power Industry (CRIEPI) and nuclear power plant manufacturers in Japan. The purpose of this program is to establish the buckling design methodology and buckling design guide under seismic loading for LMFBR components. A series of static and dynamic buckling tests and numerical analyses were carried out in this program to clarify basic buckling characteristics in shear and in bending [1]-[9].

Some analytical and experimental studies were carried out under transverse shearing loads, wherein the buckling in bending (large values of bending-to-shear stress ratio) and in shear (small values of bending-to-shear stress ratio) might occur, by Lundquist[10], Yamaki[11], Schröder[12], Galletly[13], Yuhara[14], Choi[15] and Akiyama[16].

In these studies, however, test models were nearly perfect cylinders and few studies were made for elastic-plastic buckling, therefore, it was of particular interest to evaluate the effect of geometrical imperfections on both types of buckling and to establish the interaction relation between these two types of elastic-plastic buckling experimentally.

Some experimental studies on the effect of initial imperfection were made by Tennyson[17] and Wackel[18] for axially compressed cylinders and Jullien[19] for external pressure and axial compression with cylinders by spin-casting and electrodeposition techniques.

In this paper, (1) nearly perfect cylinders with bending-to-shear stress ratios ranging from 1.2 to 5.0, (2) cylinders with intentional vertical wrinkles

(in shear) by press-working technique, where buckling load degradations were considered to be nearly same as those with the buckling mode imperfection and (3) cylinders with intentional elephant foot bulges (in bending) made also by press-working technique were tested under transverse shearing loads.

From test results, (1) the interaction relation between buckling in shear and in bending and (2) the effects of initial imperfection on both types of buckling strength were clarified and the correction factors of buckling load in shear and in bending were proposed for larger values of imperfection.

2. INTERACTION RELATION OF BUCKLING

2.1 Buckling test models

Eighteen nearly perfect cylinders as shown in Table 1 and Fig. 1, having a radius (R) of 250mm or 300mm, radius-to-thickness (R/t) and bending-to-shear stress ratios (H/R) ranged from 50 to 200 and 1.2 to 5.0, respectively, were examined under transverse shearing loads. In these model numbers, the first symbol indicates test temperature (R: room temperature and H: 500°C) and following numbers were radius-to-thickness ratio R/t, length-to-radius ratio L/R and bending-to-shear stress ratio H/R. These models were fabricated by rolling of austenitic 304 stainless steel plates with one weld seam along the longitudinal direction and fixed to both flanges (304 stainless steel).

Table 1 Test model geometries (1)

Model No.	Test Temp.	R mm	t mm	L/R	H/R	Wim mm
R167-1.0-1.2	RT	250	1.47	1.0	1.2	0.62
H200-1.0-1.5	500℃	250	1.20	1.0	1.5	0.53
H167-1.0-1.5	500℃	250	1.51	1.0	1.5	0.47
H125-1.0-1.5	500℃	250	1.94	1.0	1.5	0.49
H100-1.5-2.0	500℃	300	2.91	1.5	2.0	1.00
H100-1.5-2.5	500℃	300	2.91	1.5	2.5	0.79
H100-1.5-3.0	500℃	300	2.91	1.5	3.0	1.01
H100-2.0-2.0	500℃	300	2.91	2.0	2.0	1.47
H100-2.0-2.5	500℃	300	2.91	2.0	2.5	0.98
H150-1.5-2.0	500℃	300	1.89	1.5	2.0	1.18
H150-1.5-2.5	500℃	300	1.89	1.5	2.5	0.91
H150-2.0-2.0	500℃	300	1.89	2.0	2.0	1.32
H100-2.0-3.0	500℃	300	3.01	2.0	3.0	1.10
H100-2.0-5.0	500℃	300	3.01	2.0	5.0	0.98
H50-2.0-2.0	500℃	300	5.87	2.0	2.0	0.60
H50-2.0-3.0	500℃	300	5.94	2.0	3.0	0.96
H50-2.0-5.0	500℃	300	5.91	2.0	5.0	1.28
H50-1.5-1.5	500℃	300	5.86	2.0	1.5	0.54

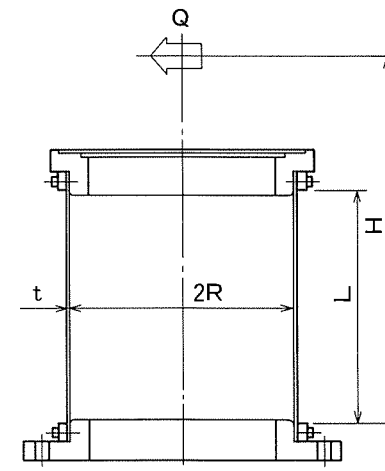

Fig.1 Configuration of test model

The buckling test setup was illustrated in Fig. 2, where test model was fixed horizontally, and transverse shearing loads were applied by a screw jack or a hydraulic actuator under the displacement control condition. The bending-to-shear stress ratios were adjusted by moving the test model with an adapter attached at the loading side of the cylinder.

For elevated temperature tests, models were controlled to 500°C±10°C at 20 measuring points by electric heaters inside a test cylinder.

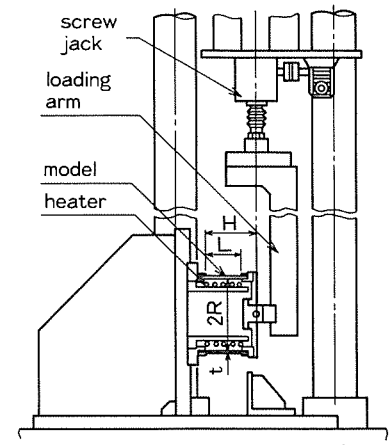

Fig.2 Buckling test setup

2.2 Test results and discussion

Test results in Table 2 showed that buckling in shear was occurred for cylinders with bending-to-shear stress ratios of 1.2 and 1.5, and buckling in bending for those of 2.5 to 5.0. For all radius-to-thickness ratios tested here, the buckling modes in shear and in bending were mixed for bending-to-shear stress ratio of 2.0.

Typical measured buckling modes were shown in Fig. 3 along the circumferential and longitudinal directions. In model No. H100-2.0-2.0 and H50-2.0-2.0, two types of buckling were observed, one was buckling in shear characterized by longitudinal skewed wrinkles near the maximum shear stress side (270°) and the other was buckling in bending characterized, in this case, by so called elephant foot bulges near the maximum compressive stress side (180°).

The detailed distributions of buckling mode in bending, which were traced along the longitudinal direction as reference data for intentional imperfect cylinders described in §4, are illustrated in Fig. 4. From these measurements, the peak position of the buckling mode was about 35mm for R/t=100, accordingly the wave length of buckling mode Lcr was 70mm, and this wave length increased with decreasing radius-to-thickness ratio (Lcr=130mm for R/t=50).

Table 2 Results of buckling test in shear and in bending

Model No.	σy kgf/mm²	Qexp tonf	δcr mm	Mode	Qs tonf	Qb tonf	Q tonf	Qexp/Qs	Qexp/Qb	Qexp/Q
R167-1.0-1.2	30.5	17.3	0.84	S	14.7	23.4	14.5	1.17	0.74	1.20
H200-1.0-1.5	17.2	8.20	0.57	S	7.28	9.19	6.90	1.13	0.89	1.19
H167-1.0-1.5	17.0	11.5	0.83	S	10.2	12.6	9.63	1.12	0.91	1.19
H125-1.0-1.5	16.4	14.5	0.94	S	14.1	17.0	13.2	1.03	0.85	1.10
H100-1.5-2.0	18.6	28.7	3.11	FS	28.4	26.8	24.0	1.01	1.07	1.20
H100-1.5-2.5	18.6	23.3	2.38	F	28.4	21.5	20.5	0.82	1.09	1.13
H100-1.5-3.0	18.6	20.0	2.01	F	28.4	17.9	17.5	0.71	1.12	1.14
H100-2.0-2.0	18.6	27.6	3.93	FS	27.2	26.8	23.5	1.02	1.03	1.17
H100-2.0-2.5	18.6	23.7	3.18	F	27.2	21.5	20.3	0.87	1.10	1.17
H150-1.5-2.0	18.5	16.0	1.61	FS	15.2	15.3	13.3	1.05	1.04	1.20
H150-1.5-2.5	18.5	13.7	1.57	F	15.2	12.3	11.6	0.90	1.12	1.19
H150-2.0-2.0	18.5	15.3	1.83	FS	14.2	15.3	12.8	1.08	1.00	1.19
H100-2.0-3.0	19.0	22.1	4.06	F	28.9	19.0	18.5	0.76	1.17	1.19
H100-2.0-5.0	19.0	13.2	3.67	F	28.9	11.4	11.4	0.46	1.16	1.16
H50-2.0-2.0	13.6	54.0	18.0	FS	50.0	44.9	41.0	1.08	1.20	1.32
H50-2.0-3.0	13.6	39.2	9.07	F	50.7	30.3	29.9	0.77	1.29	1.31
H50-2.0-5.0	13.6	23.4	9.73	F	50.4	18.1	18.1	0.46	1.29	1.29
H50-1.5-1.5	13.6	62.5	17.6	S	50.6	59.8	47.1	1.23	1.04	1.33

Mode S : Shear, F : Bending, FS : Bending+Shear

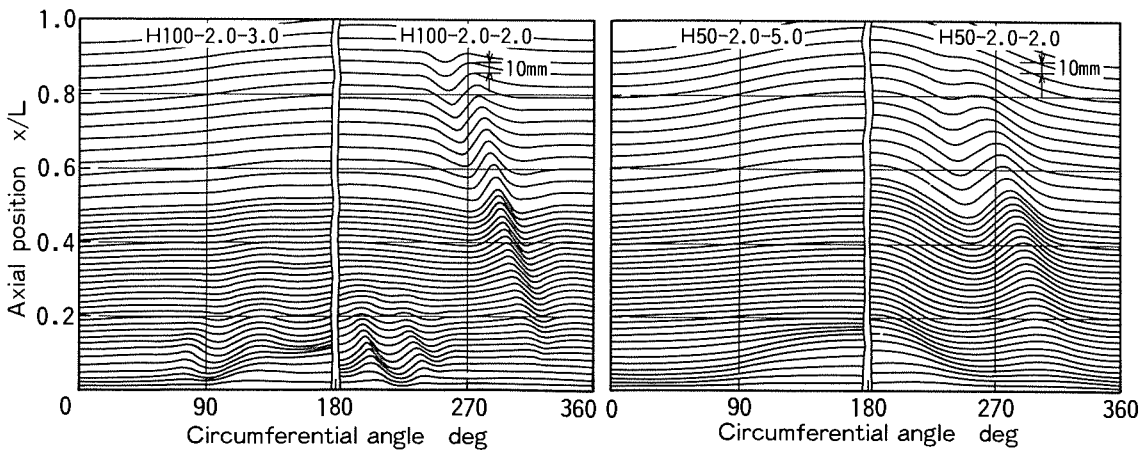

Fig.3 Distribution of measured buckling mode in shear and in bending

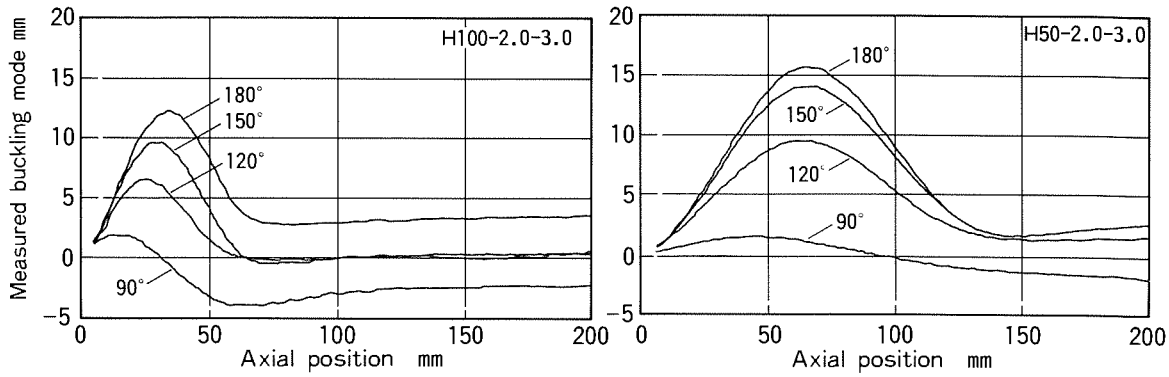

Fig.4 Axial distribution of buckling mode in bending

Table 2 also summarized buckling loads estimation in shear Qs and in bending Qb proposed in the interim buckling design guide[1] and given in Eqs. (1) and (2). Experimental buckling loads Qexp normalized by above mentioned Qs and Qb are shown in Fig. 5, where open symbols and solid symbols are buckling mode in bending and in shear, respectively. The numbers in this figure are bending-to-shear stress ratios. A week interaction was observed between buckling in shear and in bending and this interaction can be related by the 5th power law expressed in terms of Eq. (3).

$$\tau_{cr}^{e}=0.8\frac{4.82}{(L/\sqrt{Rt})^2}\sqrt{1+0.0239(L/\sqrt{Rt})^3}\cdot\frac{Et}{R}$$

$$(\tau_{cr}^{p}/\tau_{cr}^{e})+(\sqrt{3}\,\tau_{cr}^{p}/1.27S_y)^2=1$$

$$Q_s=\pi Rt\,\tau_{cr}^{p} \qquad (1)$$

$$\sigma_{cr}^{e}=0.6(1-0.731(1-\exp(-\frac{1}{16}\sqrt{R/t})))\cdot\frac{Et}{R}$$

$$(\sigma_{cr}^{p}/\sigma_{cr}^{e})+(\sigma_{cr}^{p}/1.27S_y)^2=1$$

$$Q_b=\pi R^2 t\,\sigma_{cr}^{p}/H \qquad (2)$$

$$(Q/Q_s)^5+(Q/Q_b)^5=1 \qquad (3)$$

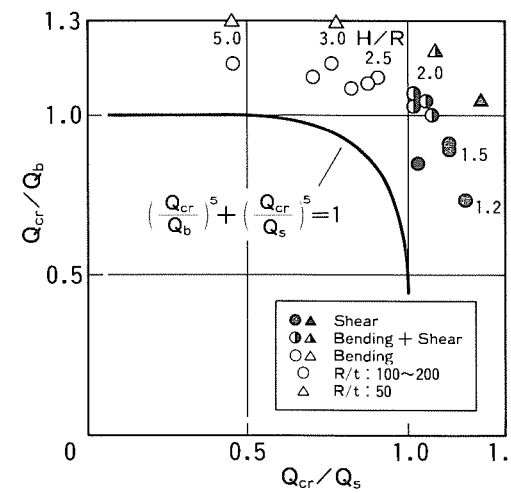

Fig.5 Interaction between buckling in shear and in bending

3. IMPERFECTION EFFECT ON BUCKLING IN SHEAR

3.1 Buckling test models

Buckling tests focused on the evaluation of imperfection effect on buckling in shear were carried out using nine test models presented in Table 3. In this table, the last four models were nearly perfect cylinders (same as in Table 1) used as reference data. The radius of these cylinders was 250mm with radius-to-thickness ratios (R/t) of 125, 167 and 200, length-to-radius ratio (L/R) of 1.0 and bending-to-shear stress ratios (H/R) of 1.2 and 1.5, respectively. In these model numbers, test temperature (R: room temperature and H: 500°C)

Table 3 Test model geometries (2)

Model No.	Test Temp.	R mm	t mm	L/R	H/R	Wave No.	Wim/t
R167-W12-T	RT	250	1.47	1.0	1.2	12	0.90
R167-W12-2T	RT	250	1.47	1.0	1.2	12	2.01
R167-W12-4T	RT	250	1.50	1.0	1.5	12	3.81
R167-W6-2T	RT	250	1.47	1.0	1.2	6	1.71
R167-AX	RT	250	1.51	1.0	1.2	AX	2.65
H200-W12-2T	500℃	250	1.20	1.0	1.5	12	1.93
H167-W12-2T	500℃	250	1.50	1.0	1.5	12	1.91
H167-W12-4T	500℃	250	1.50	1.0	1.5	12	3.89
H125-W10-2T	500℃	250	1.93	1.0	1.5	10	2.07
R167-1.0-1.2	RT	250	1.47	1.0	1.2	Nearly Perfect	
H200-1.0-1.5	500℃	250	1.20	1.0	1.5	Nearly Perfect	
H167-1.0-1.5	500℃	250	1.51	1.0	1.5	Nearly Perfect	
H125-1.0-1.5	500℃	250	1.94	1.0	1.5	Nearly Perfect	

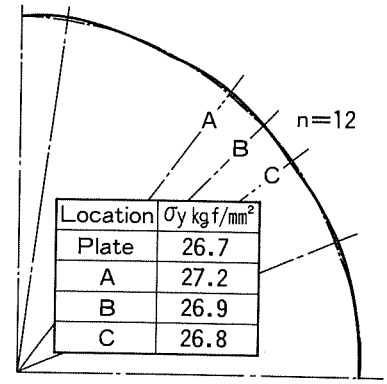

Fig.6 Cross sectional view of cylinder

was indicated by the first symbol as in Table 1 and the following numbers were R/t, imperfection modes (W6, W10, W12: circumferential wave numbers of 6, 10, 12 and AX: axisymmetric imperfection) and imperfection peak-to-peak amplitudes normalized by wall thickness.

These imperfect cylinders were fabricated by press-working of austenitic 304 stainless steel plates using a template containing the desired wave length and amplitude that was given by Eq. (4) with one welded seam along the longitudinal direction. The wave number of vertical wrinkles, in this case 10 (R/t=125) or 12 (R/t=167 and 200), was nearly identical with the dominant buckling mode for corresponding nearly perfect cylinders. A cylinder with wrinkles having wave number of 6 (one-half wave number of the buckling mode) was tested to evaluate the effect of the wave length on the buckling load. Measured shape imperfections presented in Fig. 7 showed that these imperfect cylinders were satisfactory for the buckling tests.

$$W=\frac{Wim}{2}\cos(n\theta)\sin\left(\frac{\pi x}{L}\right) \qquad \text{n : circumferential wave number} \qquad (4)$$

The mechanical property tests using small test pieces cut out from the imperfect cylinder showed that 0.2% proof stress and stress-strain relation seemed to be almost same as those for nearly perfect one as shown in Fig. 6.

A cylinder with axisymmetric imperfections, which may be caused by the operating axial temperature distribution in a reactor vessel, was machined to a prescribed profile (diameter at one end was 500mm and increased to 504mm at the other end).

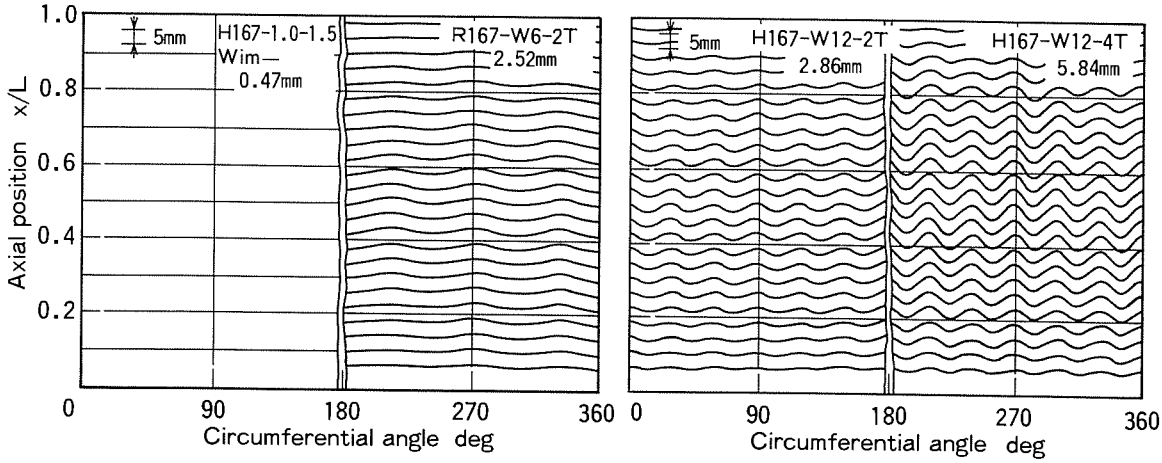

Fig.7 Distributions of typical measured imperfection

3.2 Test results and discussion

Examples of load-displacement curve for cylinders (R/t=167) are illustrated in Fig. 8. The buckling load reduction, summarized in Table 4 with test results, was 9% (Wim=T, RT), 20% (Wim=2T, RT), 15%-17% (Wim=2T, HT), 28% (Wim=4T, RT) and 26% (Wim=4T, HT), respectively as shown in Fig. 9, and load-displacement curves with buckling mode wrinkles showed gentle load decreasing rate in the post buckling region as shown in Fig. 8.

From these tests, it was emphasized that post buckling behavior in shear was quite stable and the shear buckling was less imperfection sensitive compared with an axial one. Examples of buckling mode in these tests are shown in Fig. 10, where the dominant wave number of the buckling mode was 10-12 (R/t=200) and 8-10 (R/t=125), respectively, as expected before. By comparing experimental buckling loads Qexp with estimated Qs, ratios of Qexp/Qs were 1.03-1.17 (nearly perfect), 1.07 (buckling mode, Wim=T), 0.88-0.96 (buckling mode, Wim=2T), 1.09 (one-half buckling mode, Wim=2T), 0.83 (buckling mode, Wim=4T) and 1.18 (axisymmetric) as shown in Table 4.

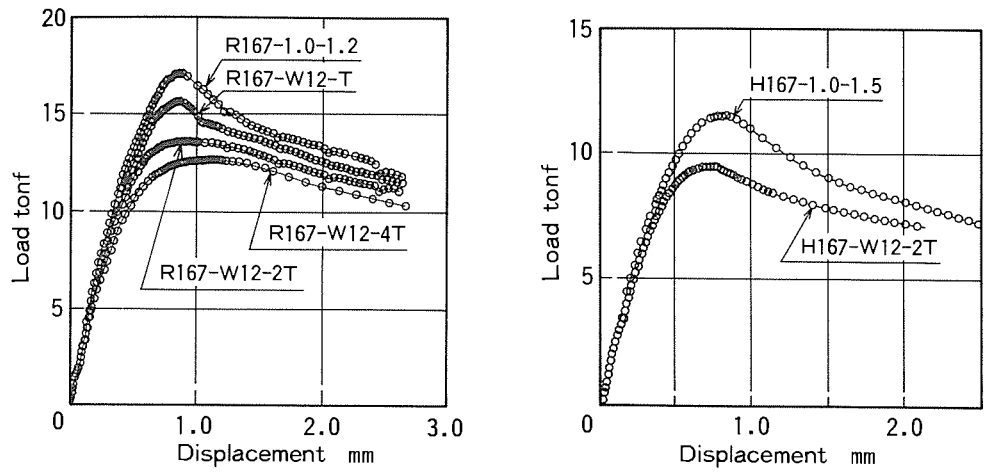

Fig.8 Load-displacement curves for nearly perfect and imperfect cylinders

Table 4 Results of buckling test in shear with imperfection

Model No.	σy kgf/mm²	Qexp tonf	δcr mm	η	Qs tonf	Qexp/Qs
R167-W12-T	30.5	15.8	0.83	0.91	14.7	1.07
R167-W12-2T	30.5	13.8	0.90	0.80	14.7	0.94
R167-W12-4T	30.6	12.7	1.06	0.72	15.3	0.83
R167-W6-2T	30.5	16.1	1.01	0.93	14.7	1.09
R167-AX	24.3	16.1	0.81	—	13.6	1.18
H200-W12-2T	17.2	6.95	0.54	0.85	7.28	0.96
H167-W12-2T	17.0	9.49	0.73	0.83	10.1	0.94
H167-W12-4T	17.0	8.42	0.84	0.74	10.1	0.83
H125-W10-2T	16.4	12.3	0.85	0.85	13.9	0.88
R167-1.0-1.2	30.5	17.3	0.84	1.00	14.7	1.17
H200-1.0-1.5	17.2	8.20	0.57	1.00	7.28	1.13
H167-1.0-1.5	17.0	11.5	0.83	1.00	10.2	1.12
H125-1.0-1.5	16.4	14.5	0.94	1.00	14.1	1.03

η : Buckling load reduction

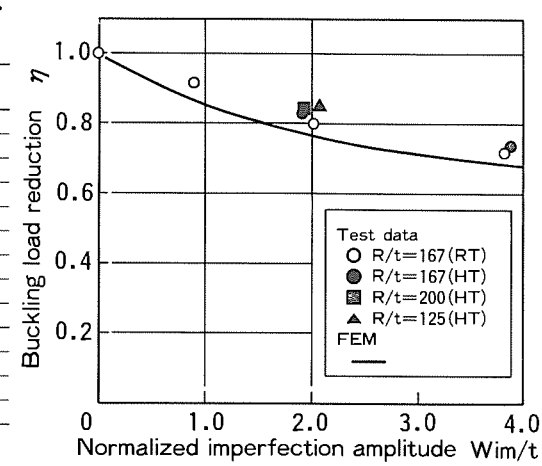

Fig.9 Buckling load reduction in shear

These results clarified that there existed some margin in Qs for nearly perfect cylinders (about 3%-17%) and even for the imperfect cylinder (about

7%) whose imperfection amplitude was within the wall thickness. This margin was resulted due to the conservative estimations of the elastic shear buckling stress and the elastic-plastic interaction relation. It was also clarified that the buckling load reduction was influenced significantly by the circumferential wave length, however, the axisymmetric imperfection tested here did not affect the buckling load compared with that for a nearly perfect cylinder. Based on the test results discussed above, we proposed the buckling load correction factor in shear for larger values of imperfection as plotted in Fig. 11.

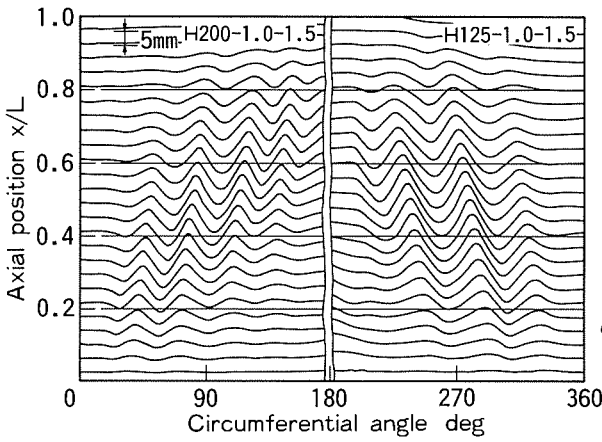

Fig.10 Measured shear buckling modes for nearly perfect cylinders

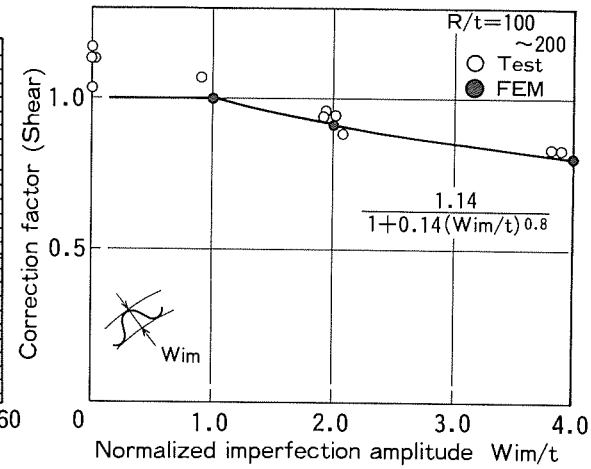

Fig.11 Buckling load correction factor (shear)

4. IMPERFECTION EFFECT ON BUCKLING IN BENDING

4.1 Buckling test models

Table 5 shows eight imperfect test cylinders, having a radius of 300mm, R/t of 100 and 50, L/R of 2.0 and H/R of 3.0, where dominant buckling mode was bending under transverse shearing loads, with the last two reference models. In model numbers, rather complicated with many parameters, the first block shows the test temperature (500°C) and R/t. The second block, 0.5H or 1.0F for example, shows imperfection peak-to-peak amplitude normalized by the wall thickness and imperfection mode as shown in Fig. 12 (H: elephant-foot bulge in the compressive stress side, F: axisymmetric mode whose cross section is an aforementioned elephant-foot bulge). The third block indicates the imperfection wave length normalized by a wave length of an elephant-foot bulge.

Table 5 Test model geometries (3)

Model No.	Test Temp.	R mm	t mm	L/R	H/R	Mode	Lc mm	Wim/t
H100-0.5H-L	500℃	300	3.01	2.0	3.0	B	70	0.52
H100-1.0H-L	500℃	300	3.01	2.0	3.0	B	70	1.07
H100-0.5F-L	500℃	300	3.01	2.0	3.0	A	70	0.50
H100-1.0F-L	500℃	300	2.99	2.0	3.0	A	70	1.04
H50-0.5H-L	500℃	300	5.93	2.0	3.0	B	130	0.51
H50-0.5F-L	500℃	300	5.87	2.0	3.0	A	130	0.53
H50-0.5F-0.5L	500℃	300	5.82	2.0	3.0	A	65	0.50
H50-0.5F-1.5L	500℃	300	5.87	2.0	3.0	A	195	0.57
H100-2.0-3.0	500℃	300	3.01	2.0	3.0	Nearly Perfect		
H50-2.0-3.0	500℃	300	5.94	2.0	3.0	Nearly Perfect		

Mode A : Axisymmetric, B : Buckling mode,
Lc: Imperfection wave length

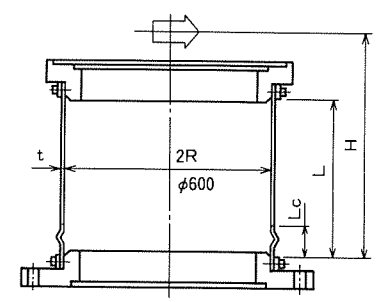

Fig.12 Schematic view of axisymmetric imperfection

These imperfect cylinders with intentional wave were fabricated by press-working technique of 304 austenitic stainless steel plates as stated in §3. The hardness check for test pieces, cut out from the imperfect cylinder, showed that 0.2% proof stress was not affected very much by this process.

Cylinders of H50-0.5F-0.5L (a half wave length) and H50-0.5F-1.5L (1.5 times wave length) were tested to evaluate the effect of the wave length on the buckling load. Typical measured shape imperfections evaluated along the longitudinal direction are shown in Fig. 13 and these distributions agreed well with the buckling modes given in Fig. 4.

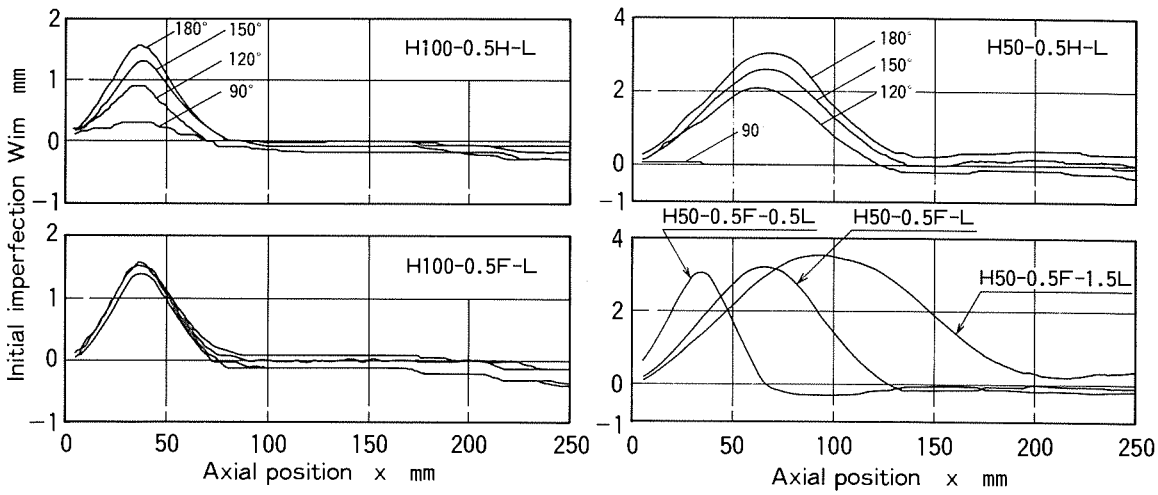

Fig.13 Distributions of measured imperfection along the longitudinal direction

4.2 Test results and discussion

Figure 14 shows typical load-displacement relations for nearly perfect and imperfect cylinders with R/t of 100 and 50. The load-displacement curves for cylinders with R/t=50 revealed large nonlinearity before buckling and very stable post buckling behavior, which may be characterized by a plastic collapse rather than buckling. For cylinders with R/t=100, load-displacement curves with imperfection showed gentle load decreasing rate in the post buckling region same as shear buckling in Fig. 8.

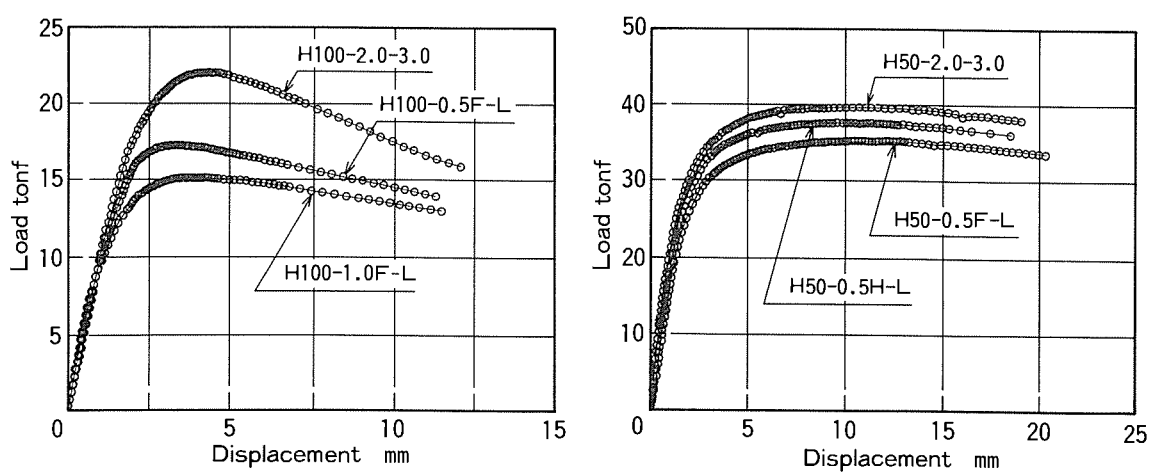

Fig.14 Load-displacement curves for nearly perfect and imperfect cylinders

Table 6 summarizes buckling load Qexp and buckling displacement δcr associated with the buckling load degradation compared with nearly perfect cylinders and estimated buckling loads in bending Qb obtained from Eq. (2). The buckling load reductions for R/t=100 with elephant foot bulge were 13% (Wim=0.5T) and 20% (Wim=T), nearly twice as large as those in shear, and therefore it was considered that buckling in bending was rather imperfection sensitive as compared to the case of shear. For axisymmetric imperfections, these values were 22% (Wim=0.5T) and 31% (Wim=T) for R/t=100 as shown in Fig. 15. For imperfect cylinders with R/t=50, which were expected to be less imperfection sensitive because of increasing plasticity, these values were 4% (Wim=0.5T, buckling mode) and 9% (Wim=0.5, axisymmetric mode).

Table 6 Results of bending buckling test with imperfection

Model No.	σy kgf/mm²	Qexp tonf	δcr mm	η	Qb tonf	Qexp/Qb
H100-0.5H-L	19.0	19.2	3.29	0.87	18.9	1.01
H100-1.0H-L	19.0	17.6	3.96	0.80	18.9	0.93
H100-0.5F-L	19.0	17.2	3.45	0.78	18.9	0.91
H100-1.0F-L	19.0	15.2	3.77	0.69	18.8	0.81
H50-0.5H-L	13.6	37.6	10.1	0.96	30.3	1.24
H50-0.5F-L	13.6	35.3	10.8	0.91	29.9	1.18
H50-0.5F-0.5L	13.6	36.4	10.3	0.95	29.7	1.23
H50-0.5F-1.5L	13.6	37.1	10.3	0.96	29.9	1.24
H100-2.0-3.0	19.0	22.1	4.06	1.00	19.0	1.17
H50-2.0-3.0	13.6	39.2	9.07	1.00	30.3	1.29

η : Buckling load reduction

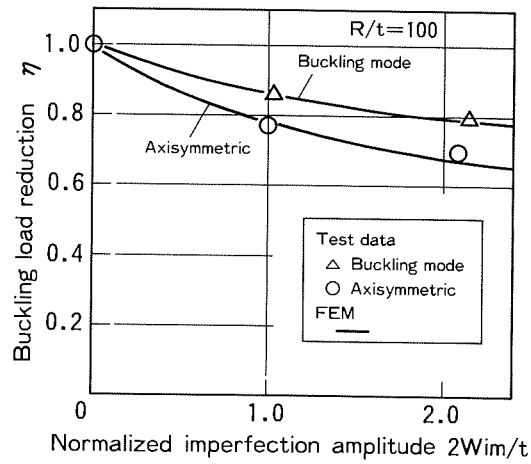

Fig. 15 Buckling load reduction in bending

Ratios of experimental buckling load Qexp to Qb for R/t=100 in Table 6 were 1.17 (nearly perfect), 1.01 (Wim=0.5T, buckling mode), 0.93 (Wim=T, buckling mode), 0.91 (Wim=0.5T, axisymmetric) and 0.81 (Wim=T, axisymmetric). For R/t=50, these values were 1.24 (Wim=0.5T, buckling mode) and 1.18 (Wim=0.5T, axisymmetric), where large margin was recognized in Qb because of the conservative estimation of buckling loads in highly plastic region like plastic collapse. The buckling load reductions were 9% for Lc=Lcr, 5% for Lc=0.5Lcr and 4% for Lc=1.5Lcr, where Lc and Lcr were wave length of imperfection and buckling mode, respectively, and the minimum value was attained at Lc=Lcr as shown in Fig. 16.

Based on these results, some margin was recognized in Qb for nearly perfect cylinders, those were 17% (H100-02.0-3.0) for R/t=100 and 29% (H50-2.0-3.0) for R/t=50, and even for the imperfect cylinder with buckling mode imperfection, 1% (H100-0.5H-L) for R/t=100 and 24% (H50-0.5H-L) for R/t=50, whose imperfection amplitudes were within one-half the wall thickness. This margin increased with decreasing radius-to-thickness ratio because of the reason stated above.

From test results discussed above, we proposed the buckling load correction factor in bending for larger values of imperfection as presented in Fig. 17.

5. NUMERICAL ANALYSIS

Numerical calculations were carried out with general-purpose finite element analysis codes MARC and ABAQUS. For buckling in shear, it was clarified that the buckling load reduction of cylinders with buckling mode imperfections,

which may be considered as the worst one, was approximately equal to that for with vertical wrinkles of same wave numbers as the buckling mode. Calculated buckling load reductions in shear and in bending are shown in Figs. 9 and 15, respectively, and these values agreed well with test results.

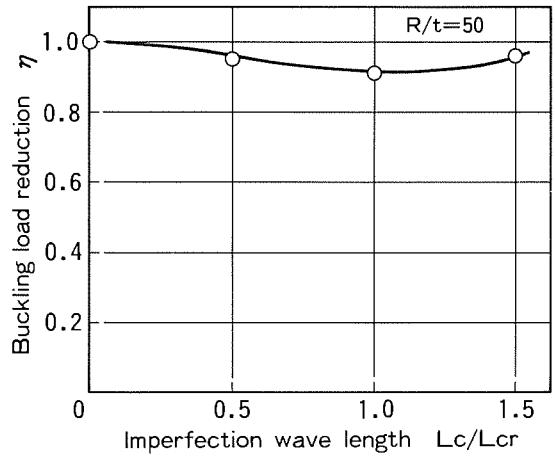

Fig.16 Effect of imperfection wave length on buckling in bending

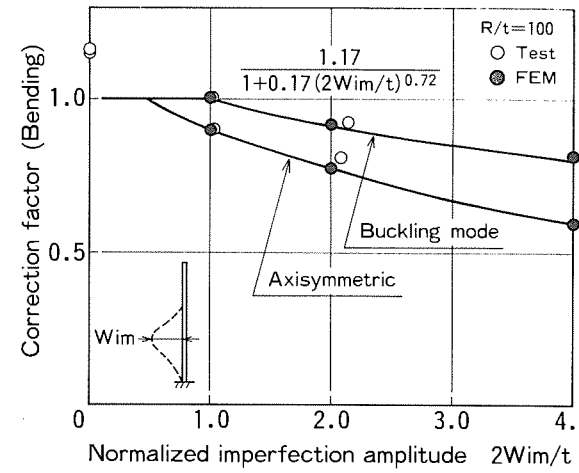

Fig.17 Buckling load correction factor (bending)

6. BUCKLING LOAD CORRECTION FACTORS

From test results described in §3 and §4, Eqs. (1) and (2) used for estimating buckling loads in shear and in bending, respectively, were expected to be valid even for cylinders with the worst imperfection like the buckling mode in shape when imperfection amplitudes were within the wall thickness (in shear) and within one-half the wall thickness (in bending). For larger values of imperfection mentioned above, we proposed the following empirical relations for buckling load correction factors expressed by Eq. (5) (in shear) and Eq. (6) (in bending) for the interim buckling design guide of LMFBR. Imperfection amplitudes were defined in this paper, for simplicity, by measuring those within a gauge length of the buckling wave length, namely Lgθ (in shear) or Lgx (in bending) given below.

$$\text{(Correction factor in shear)} = \frac{1.14}{1+0.14(\mathrm{Wim}/t)^{0.8}} \quad \text{for Wim} \geq t$$

$$\text{where} \quad L_{g\theta} = 2\,(Rt)^{0.25}\,L^{0.5} \tag{5}$$

$$\text{(Correction factor in bending)} = \frac{1.17}{1+0.17(2\mathrm{Wim}/t)^{0.72}} \quad \text{for 2Wim} \geq t$$

$$\text{where} \quad L_{gx} = 4\,(Rt)^{0.5} \tag{6}$$

7. CONCLUSIONS

Elastic-plastic buckling tests for nearly perfect cylinders and cylinders with intentional imperfection made by press-working technique were conducted

subjected to transverse shearing loads. The following conclusions concerning the interaction relation between buckling strength in bending and in shear and imperfection effect on these two types of buckling were drawn.

1. Based on the test result of nearly perfect cylinders with bending-to-shear stress ratios (H/R) ranging from 1.2 to 5.0, buckling modes were observed in shear for small values of H/R (1.2 and 1.5), in bending for large values of H/R (over 2.5) and in mixed modes for H/R=2.0.
2. Comparing these test results with estimated buckling loads in shear Qs and in bending Qb given in the interim buckling design guide of LMFBR, a week interaction was observed in these types of buckling and this relation may be approximated by the 5th power law.
3. Shear buckling tests with intentional imperfection showed that buckling load reductions were 9% (Wim=T), 15%-20% (Wim=2T) and 26%-28% (Wim=4T) for buckling mode imperfections and these values were greatly affected by the imperfection wave length.
4. Load-displacement curves were quite stable in shear buckling and showed gentle load decreasing rate in the post buckling region for cylinders with buckling mode imperfections.
5. Buckling load reductions in bending for imperfect cylinders, which were 13% (Wim=0.5T) and 20% (Wim=T) with elephant foot bulges, were nearly twice as large as those in shear, therefore it was clarified that buckling in bending was rather imperfection sensitive than buckling in shear.
6. Load-displacement curves for R/t=50 showed large nonlinearity before buckling and quite stable post buckling behavior, which may be characterized by a plastic collapse rather than buckling.
7. By comparing experimental buckling loads with Qs and Qb, some margin was recognized in Qs and Qb for even imperfect cylinders with Wim=T (in shear) and Wim=0.5T (in bending).
8. Buckling load correction factors in shear and in bending were proposed for larger values of imperfections for the interim buckling design guide of LMFBR.

ACKNOWLEDGMENT

This study was carried out as part of the project of the Ministry of International Trade and Industry, titled "Verification Tests of Fast Breeder Reactor Technology", which has been conducted since 1987.

Authors gratefully acknowledge the helpful discussion of Prof. H. Akiyama and Prof. H. Ohtsubo (University of Tokyo) and Prof. Yamada (Tohoku University) throughout the course of this work.

REFERENCES

1. Akiyama, H. et al. Outline of the Seismic Buckling Design Guideline of FBR - A tentative Draft, Nuclear Engineering and Design (to be published)
2. Akiyama, H. et al. 1991. Outline of the Seismic Buckling Design Guideline of FBR - A tentative Draft. 11th SMiRT Vol.E : 239
3. Matsuura, S. et al. 1991. Buckling Strength Evaluation of FBR Main Vessels under Lateral Seismic Loads. 11th SMiRT Vol.E : 269
4. Hagiwara. Y. et al. 1991. Seismic Margin Evaluation of FBR Main Vessels, 11th SMiRT Vol.E : 455
5. Kawamoto, Y. et al. 1991. Reduction of Seismic Response of Shell Structures with Nonlinear Deformation Characteristics, 11th SMiRT Vol.E : 257
6. Kokubo, K. et al. 1991. Corroboration of Dynamic Characteristics of FBR

Main Vessels by Pseudo-dynamic and Dynamic Buckling Experiments. 11th SMiRT Vol.E : 251
7. Ogiso, S. et al. 1991. The State of the Inelastic Shear Buckling Analysis, and Its Application to Low Cycle Fatigue Estimation. 11th SMiRT Vol.E : 293
8. Murakami, T. et al. 1991. The Effect of Geometrical Imperfection on Shear Buckling Strength of Cylindrical Shells. 11th SMiRT Vol.E : 287
9. Murakami, T. et al. 1991. Static and Dynamic Buckling Characteristics of Imperfect Cylindrical Shells under Transverse Shearing Loads, Buckling of Shell Structures, on Land, in the Sea and in the Air (edited by J.F.Jullien, Elsevier Applied Science) : 391
10. Lundquist, E.E. 1935. Strength Tests of Thin-walled Duralumin Cylinders in Combined Transverse Shear and Bending. NACA TN-523
11. Yamaki, N. 1984. Elastic Stability of Circular Cylindrical Shells. North-Holland
12. Schröder V.P. 1972. Über die Stabilität der querkaftbelasteten dünnwandigen Kreiszylinderschale. ZAMM 52 : T145
13. Galletly, G.D. et al. 1985. Plastic Buckling of Short Vertical Cylindrical Shells Subjected to Horizontal Edge Shear Loads. J. of Pressure Vessel Technology. Vol.107 : 101
14. Yuhara, T. et al. 1987. Recent Experimental Research for Buckling Design Method of FBR Component. 2nd International Seminar on Design Codes and Structural Mechanics (Lausanne-Switzerland).
15. Choi, H.S. et al. 1986. Failure Tests of Cantilevered Cylindrical Shells under a Transverse Load. J. of Structural and Construction Engineering. Vol.369 : 60
16. Akiyama, H. 1987. Buckling Tests of Steel Cylindrical Shells Subjected to Combined Bending and Shear. J. of Structural and Construction Engineering. Vol.371 : 44
17. Tennyson, R.C. et al. 1969. Buckling of Axisymmetric Imperfect Circular Cylindrical Shells under Axial Compression. AIAA Journal. Vol.7 : 2127
18. Wackel, N. et al. 1984. Experimental Studies on the Instability of Cylindrical Shells with Initial Geometric Imperfections. ASME PVP-Vol.89 : 33
19. Jullien, J.F. et al. 1991. Towards an Optimal Shape of Cylindrical Shell Structures under External Pressure. Buckling of Shell Structures, on Land, in the Sea and in the Air (edited by J.F. Jullien, Elsevier Applied Science) : 21